Optica Applicata, Vol. XX, No. 4, 1990

Application of a spherical holographic optical element as a Fourier transform lens*

E. JAGOSZEWSKI, S. GŁADYSZ

Institute of Physics, Technical University of Wrocław, Wybrzeże Wyspiańskiego 27, 50–370 Wrocław, Poland.

A. TALATINIAN**

University of Aleppo, Syria.

The holographic optical element recorded on a spherical substrate is investigated as the Fourier transform holographic lens. For recording the HOE a plane reference wave and an object spherical wave are interfered on-axis. Now, if the various spatial Fourier components are identified as plane waves propagating in different directions, then such a holographic lens can be used as a Fourier transform lens, since the complex field distribution across any plane is Fourier analysed.

1. Introduction

In this paper, a configuration for performing the Fourier transform operation by a spherical holographic lens is considered.

This problem has been studied because of a very interesting property of spherical holographic elements offering a possibility of eliminating the offence against the sine condition at a spherical position of the object. However, this property will be considered in a detailed way in the next paper being now prepared for publication.

The spherical holographic lens, compared to a conventional thin lens, can be less expensive in mass production and very useful for many applications in various domains of science and technology. A holographic lens is said to be isoplanatic if it is space-invariant, i.e., if the image of a point-source preserves its functional form when changing the point-source location. Analysis of the diffracted waves shows that, if the reconstructing source is situated at a position different from that of the reference source, the holographic image occurs with aberrations at a position different from that of the object.

In this paper, a spherical in-line hologram is recorded by the two waves: a spherical and a plane one. The paraxial position of the holographic images of an object point-source is described by the well-known imaging lens formula. For

* This work has been sponsored by the CPBP 01.06 Research Programme.

** Present address: Institute of Physics, Technical University of Wrocław, Wybrzeże Wyspiańskiego 27, 50–370 Wrocław, Poland.

realizing the Fourier transform operation, the focusing properties are used, and the reconstruction wave is a plane wave which represents a spatial frequency component of an angular spectrum. If the direction of the reconstruction wave is parallel to the optical axis, then the images are the focal points of the hologram and determine location of its focal-planes. We say that the real image (conjugate image) reconstructed by the central plane wave is the dc component of the spatial spectrum. In the case of sloped reconstruction beams, at the angle α_C (different from zero) with the optical axis, we obtain the images in the focal plane in different positions which describes the spatial frequencies of the examined input transparency.

2. Holographic Fourier transform lens

The two-dimensional Fourier transform permits studying of the structure of an object in the spatial frequency domain. It is well known that a thin lens acts as a Fourier transformer of spatial distributions providing the Fourier transform relationship between the complex amplitude in its front and back focal planes. The transform actually effectively decomposes an illuminating light wave into component plane waves whose directions correspond to its spatial frequencies. The components can be analysed in a similar way as by the conventional thin refractive lens [1].

The focusing properties of a spherical hologram are considered in such a way that the reconstructing plane waves focused in the image space are investigated in order to determine the Fourier transform of the object transmittance. When illuminated by a coaxial plane wave, the object produces an angular spectrum of the diffracted plane waves which represent various spatial frequency components of the transparency. The holographic lens focuses these wave to the points located at different distances from the axis of hologram lens. A single plane wave representing a particular spatial frequency can illuminate either the whole hologram or only a part of it [2]. In the considerations of this paper, each of these plane waves illuminates the whole holographic lens [3] in a similar fashion as in the conventional optical system. For recording, shown in Fig. 1, the object spherical wave and the reference plane are symmetrical in regard to the optical axis. Figure 2 illustrates the

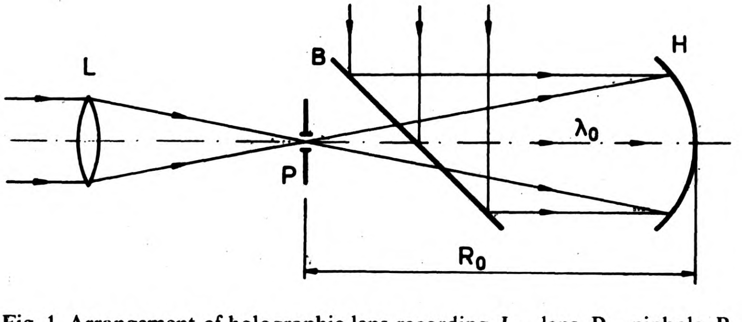

Fig. 1. Arrangement of holographic lens recording. L – lens, P – pinhole, B – beam splitter, H – spherical photolayer for hologram recording, R_0 – distance between the spherical vertex of hologram substrate and the object point-source, λ_0 – wavelength of the recording waves

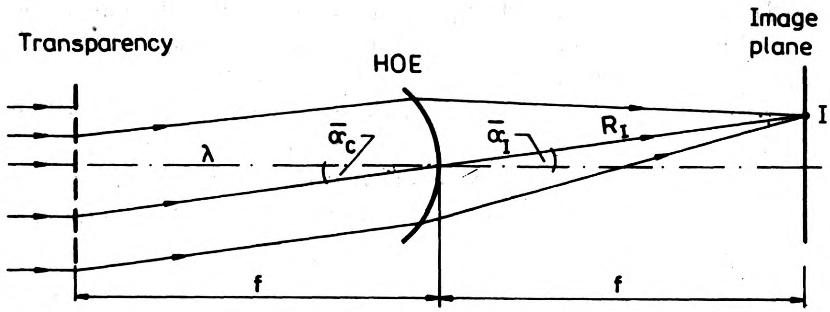

Fig. 2. Holographic optical element (HOE) as a Fourier transform lens transforming a diffracted plane wave into a spherical one. $\bar{\alpha}_C$ – incidence angle of the reconstructing wave, $\bar{\alpha}_I$ – angle of diffraction, I – image point, R_I – distance of the image point from the HOE vertex, f – focal length, λ – wavelength of the reconstructing wave

geometry for readout of the holographic lens transforming the plane wave into a spherical one which represents a particular spatial frequency of the object transmittance located in the front focal plane. If the object of amplitude transmittance $U(x_O, y_O)$ is assumed to be uniformly illuminated by a normally incident, monochromatic plane wave of wavelength $\lambda = \lambda_O$ (Fig. 2), then the distribution $U(x_f, y_f)$ of field amplitude across the back focal plane is the Fourier transform of the object transmittance

$$U(x_f, y_f) = \frac{A}{i\lambda f} \iint_{-\infty}^{\infty} U(x_O, y_O) \exp\left[-i \frac{k}{f}(x_O x_f + y_O y_f)\right] dx_O \, dy_O \tag{1}$$

where A is the amplitude of plane wave of the wave number $k = 2\pi/\lambda$, normally incident on the object plane. As shown in [4], the necessary condition for any optical element or system to perform the Fourier transform (1) is to fulfill the equation

$$U'(x, y) = U(x, y) \exp\left[-i \frac{k}{2f}(x^2 + y^2)\right] \tag{2}$$

where $f = R_O$, only for the wavelength λ equal to the wavelength λ_O.

3. Third-order aberration coefficients

For the sloped reconstructing beams, the HOE focuses the wavefronts to points in different planes located at the distances $z_I = R_I \cos\alpha_I$ from the holographic lens. Thus, Eq. (2) determining their amplitude distribution just behind the HOE in general takes the form

$$U'(x, y) = U(x, y) \exp\left[-i \frac{k}{2z_I}(x^2 + y^2)\cos\alpha_I\right]. \tag{3}$$

The procedure for obtaining aberrations of the reconstructed images is based on the

Champange theory [5], which for the spherical point hologram is described in [6]. It is well known that in this formulation there exist only three aberrations: spherical aberration, coma and astigmatism. It is also quite obvious that in the case where the direction of the reconstructing wave coincides with the reference wave of this hologram one can find an unaberrated image point which in these considerations illustrates the zero frequency of the spatial spectrum. All of the other image points are loaded with the aberrations. Therefore, the wavefront deviation from Gaussian reference sphere is given by

$$\Delta = -\frac{1}{2}\left[\frac{(x^2+y^2)^2 S}{4} - (x^2+y^2)(xC_x+yC_y)+(x^2A_x+y^2A_y+2xyA_{xy})\right] \tag{4}$$

where S, C, A are the spherical aberration, coma and astigmatism coefficients, respectively. For the spherical hologram these coefficients can be written [6] as:

$$S = \frac{1}{R_C^3} - \frac{1}{R_I^3} \pm\mu\left(\frac{1}{R_O^3} - \frac{1}{R_R^3}\right) + \frac{2}{\rho}\left[\frac{z_C}{R_C^3} - \frac{z_I}{R_I^3} \pm\mu\left(\frac{z_O}{R_O^3} - \frac{z_R}{R_R^3}\right)\right]$$
$$+\frac{1}{\rho^2}\left[\frac{z_C^2}{R_C^3} - \frac{z_I^2}{R_I^3} \pm\mu\left(\frac{z_O^2}{R_O^3} - \frac{z_R^2}{R_R^3}\right)\right],$$

$$C_x = \frac{x_C}{R_C^3} - \frac{x_I}{R_I^3} \pm\mu\left(\frac{x_O}{R_O^3} - \frac{x_R}{R_R^3}\right) + \frac{1}{\rho}\left[\frac{x_C z_C}{R_C^3} - \frac{x_I z_I}{R_I^3} \pm\mu\left(\frac{x_O z_O}{R_O^3} - \frac{x_R z_R}{R_R^3}\right)\right],$$

$$C_y = \frac{y_C}{R_C^3} - \frac{y_I}{R_I^3} \pm\mu\left(\frac{y_O}{R_O^3} - \frac{y_R}{R_R^3}\right) + \frac{1}{\rho}\left[\frac{y_C z_C}{R_C^3} - \frac{y_I z_I}{R_I^3} \pm\mu\left(\frac{y_O z_O}{R_O^3} - \frac{y_R z_R}{R_R^3}\right)\right],$$

$$\mathrm{A}_x = \frac{x_C^2}{R_C^3} - \frac{x_I^2}{R_I^3} \pm\mu\left(\frac{x_O^2}{R_O^3} - \frac{x_R^2}{R_R^3}\right),$$

$$A_y = \frac{y_C^2}{R_C^3} - \frac{y_I^2}{R_I^3} \pm\mu\left(\frac{y_O^2}{R_O^3} - \frac{x_R^2}{R_R^3}\right),$$

$$A_{xy} = \frac{x_C y_C}{R_C^3} - \frac{x_I y_I}{R_I^3} \pm\mu\left(\frac{x_O y_O}{R_O^3} - \frac{x_R y_R}{R_R^3}\right) \tag{5}$$

where $\mu = \lambda/\lambda_O$, while λ_O and λ denote the wavelengths used during recording and reconstruction, respectively.

We see that only spherical aberration and coma depend on the curvature of the hologram substrate. The radius of the hologram substrate does not influence the astigmatism.

4. Spherical holographic lens as a diffraction grating

In contradiction to conventional lens, the holographic lens is an optical element which images by diffraction and interference rather than by refraction or reflection. Suppose that two waves with a plane and a spherical wavefront interfere on a spherical photolayer. The system of interference fringes forming on the spherical substrate depends on the incidence angle of the two interfering waves. If the wavelength of the two interfering waves is λ_O, then the distance between two adjacent fringes which determine the period of the diffraction grating [7] is

$$d = \frac{\lambda_O}{\sin\alpha_R + \sin\alpha_O} \tag{6}$$

where α_R and α_O are the incidence angles of the two waves (we say reference and object waves, respectively), as shown in Fig. 3. But from Figure 3 we have:

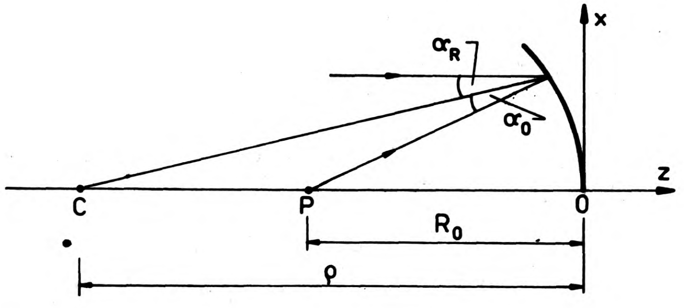

Fig. 3. Ray tracing of two waves interfering at the spherical substrate. α_R, α_O – incidence angles of the two waves (reference and object, respectively), P – axial point-source, C – center of the sphere, ρ – curvature radius of the spherical substrate, R_O – object distance from the sphere vertex

$$\sin\alpha_R = x/\rho,$$

$$\sin\alpha_O = \frac{(\rho-f)x}{\rho\sqrt{f^2+2(\rho-f)\left(\rho-\sqrt{\rho^2-x^2}\right)}}.$$

Inserting the two expressions into Eq. (6), we obtain the grating spacing of the holographic lens which depends not only on the curvature radius, but also on the coordinates (x, y) of the points at the substrate surface. We can notice that the spatial frequency of the interference fringes at the spherical substrate changes from vertex to the edge of the lens in all the radial directions in the following way:

$$\frac{1}{d} = \left[\frac{\rho-f+\sqrt{f^2+2(\rho-f)\left(\rho-\sqrt{\rho^2-x^2-y^2}\right)}}{\lambda_O\rho\sqrt{f^2+2(\rho-f)\left(\rho-\sqrt{\rho^2-x^2-y^2}\right)}}\right]\sqrt{x^2+y^2}. \tag{7}$$

The minimum value of spatial frequency of the interference fringes we can find at the edge of such a holographic lens where the minimal grating specing is expressed by the equation

$$d_{\min} = \frac{2\rho\lambda_O\sqrt{f^2+(\rho-f)\left(2\rho-\sqrt{4\rho^2-D_H^2}\right)}}{D_H\left[\rho-f+\sqrt{f^2+(\rho-f)\left(2\rho-\sqrt{4\rho^2-D_H^2}\right)}\right]} \tag{8}$$

where D_H is the diameter of this lens. Figure 4 gives the graphs of the function

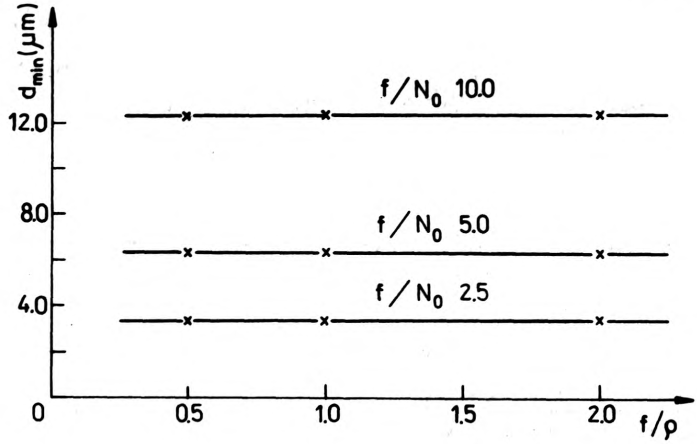

Fig. 4. Comparison between the curves of the minimal grating spacing as a function of the curvature radius of holographic lens for three different values of f-number

$d_{min} = d(\rho)$ for $\lambda_O = 632.8$ nm, $f = R_O = 100.0$ mm and three different values of the f-number, i.e., 10, 5.0 and 2.5. We see that the three curves are the straight lines parallel to each other, i.e., the minimal grating spacing of the investigated HOE is almost constant in the considered region of lens curvatures.

5. Numerical illustration and conclusion

In seeking the best recording geometry for producing the Fourier holographic lens, we considered two different approaches. In the first, the hologram is made by the two interfering waves which form the angle of $\bar{\alpha}_O = \bar{\alpha}_R = 0°$ with the optical axis of the system, as shown in Fig. 1; analogously in the second case, the holographic lens is fabricated by the object and reference waves at the same wavelength which are sloped to the axis at the angle of $\bar{\alpha}_O = \bar{\alpha}_R = 10°$. The investigations of third order aberrations in the $(x\text{–}z)$ plane were carried out, and the spherical aberration, coma and astigmatism coefficients have been calculated by assumption of the remaining parameters as follows: $R_O = 100.0$ mm, $\lambda_O = \lambda_C = 632.8$ nm with the maximum aperture of $D_H = 10.0$ mm. The plane waves propagating in different directions which represent the analysed spatial frequencies are transformed by the Fourier transform holographic lens. In the back focal plane of the lens, the images determining different spatial frequencies are formed.

Tables 1 and 2 show the values of aberration coefficients for the two different holographic lenses recorded by assuming $\bar{\alpha}_O = \bar{\alpha}_R = 0°$, and $\bar{\alpha}_O = \bar{\alpha}_R = 10°$. The coefficients were calculated at the slope of $\alpha_C = 0$ –$14°$ of the incident plane wave directions, and for three different values of curvature radius of the lens. Moreover, using Eq. (4), the third order imaging deviation can be evaluated. The wavefront deviation from the Gaussian sphere may be written as a one-dimensional function of the spherical aberration, coma and astigmatism in the form

Table 1. Third order aberration coefficients for $\bar{\alpha}_O = \bar{\alpha}_R = 0°$

$\bar{\alpha}_C$	0°			4°		
ρ	50.0	100	200	50	100	200
S	-1.8×10^{5}	-8.0×10^{-6}	-4.5×10^{-6}	-1.79×10^{-5}	-7.97×10^{-6}	-4.48×10^{-5}
C_x	0	0	0	-2.08×10^{-5}	-1.39×10^{-5}	-1.04×10^{-5}
A_x	0	0	0	-4.85×10^{-5}	-4.85×10^{-5}	-4.85×10^{-5}
$\bar{\alpha}_C$	10°			14°		
ρ	50.0	100	200	50	100	200
S	-1.76×10^{-5}	-7.82×10^{-6}	-4.4×10^{-6}	-1.72×10^{-5}	-7.65×10^{-6}	-4.31×10^{-6}
C_x	-5.05×10^{-5}	-3.37×10^{-5}	-2.53×10^{-5}	-6.83×10^{-5}	-4.56×10^{-5}	-3.42×10^{-5}
A_x	-2.97×10^{-4}	-2.97×10^{-4}	-2.97×10^{-4}	-5.68×10^{-4}	-5.68×10^{-4}	-5.68×10^{-4}

(ρ in mm)

Table 2. Third order aberration coefficients for $\bar{\alpha}_O = \bar{\alpha}_R = 10°$

α_C	0			4°		
ρ	50.0	100	200	50	100	200
S	-1.80×10^{-5}	-8.06×10^{-6}	-4.56×10^{-6}	-1.79×10^{-5}	-8.03×10^{-6}	-4.54×10^{-6}
C_x	-5.16×10^{-5}	-3.45×10^{-5}	-2.59×10^{-5}	-7.28×10^{-5}	-4.87×10^{-5}	-3.66×10^{-5}
A_x	-3.02×10^{-4}	-3.02×10^{-4}	-3.02×10^{-4}	-3.51×10^{-4}	-3.51×10^{-4}	-3.51×10^{-5}
α_C	10			14°		
ρ	50	100	200	50	100	200
S	-1.76×10^{-5}	-7.88×10^{-6}	-4.45×10^{-6}	-1.73×10^{-5}	-7.71×10^{-6}	-4.36×10^{-6}
C_x	-1.03×10^{-4}	-6.89×10^{-5}	-5.18×10^{-5}	-1.21×10^{-4}	-8.11×10^{-5}	-6.10×10^{-5}
A_x	-6.03×10^{-4}	-6.03×10^{-4}	-6.03×10^{-4}	-8.78×10^{-4}	-8.78×10^{-4}	-8.78×10^{-4}

(ρ in mm)

$$\Delta(x) = -\frac{x^4}{8\lambda_C}S(\alpha_C) + \frac{x^3}{2\lambda_C}C(\alpha_C) - \frac{x^2}{2\lambda_C}A(\alpha_C) \tag{9}$$

where:

$$S(\alpha_C) = -(\cos^3\alpha_C + \cos^3\alpha_O)\left[\frac{1}{f^3} + \frac{2}{\rho f^2} + \frac{1}{\rho^2 f}\right],$$

$$C(\alpha_C) = -(\sin\alpha_C\cos^2\alpha_C + \sin\alpha_O\cos^2\alpha_O)\left[\frac{1}{f^2} + \frac{1}{\rho f}\right],$$

$$A(\alpha_C) = -\frac{1}{f}\left[\sin^2\alpha_C\cos\alpha_C + \sin^2\alpha_O\cos\alpha_O\right],$$

and

$$f = R_O\cos\alpha_O. \tag{10}$$

In this analysis of holographic image evaluation, we have confined our attention to point imagery, and therefore we do not have five monochromatic aberrations as in conventional lens optics. Figures 5 and 6 illustrate the wavefront deviation from the Gaussian sphere in wavelengths comprehending the three aberrations given in

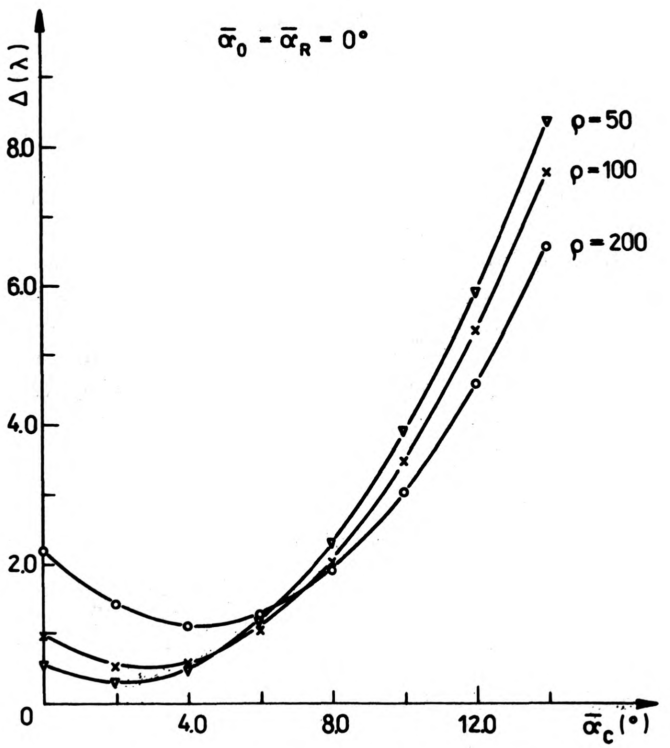

Fig. 5. Wavefront deviation in wavelengths vs the incidence angle of reconstruction beam for a holographic lens produced by waves of $\bar{\alpha}_O = \bar{\alpha}_R = 0°$

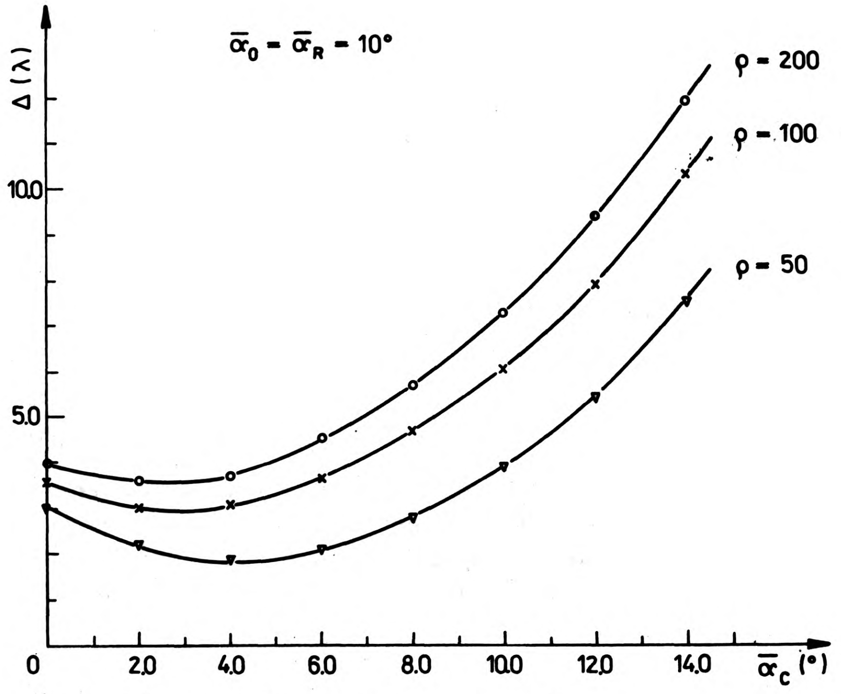

Fig. 6. The same as in Fig. 5, but for $\bar{\alpha}_O = \bar{\alpha}_R = 10°$

Tables 1 and 2, respectively. We see that one can find the best focus at different distances from the holographic lens vertex depending on the value of reconstructing wave slope angle α_C. By shifting the image focal plane in the axial direction, we can correct the imaging of spatial frequences of the investigated transparency.

At this point, it is worthwhile to compare the two different holographic Fourier transform lenses (comp. Tab. 1 and 2). A curved hologram has been used as a Fourier transformer for investigation of spatial frequency distribution. The considerations cover a wide range of spatial frequencies. It has been shown that for a special selection of the holographic lens parameters, the image points representing the spatial frequencies of an angular spectrum can be improved and explicitly corrected.

References

[1] GOODMAN J. W., *Introduction to Fourier Optics*, McGraw-Hill Book Co., New York 1968.
[2] AMITAI Y., FRIESEM A. A., J. Opt. Soc. Am. A **5** (1988), 702.
[3] JAGOSZEWSKI E., TALATINIAN A., Opt. Appl. **19** (1989), 75.
[4] JAGOSZEWSKI E., *Holografia optyczna* (in Polish), PWN, Warszawa 1986.
[5] CHAMPAGNE E. B., *A qualitative and quantitative study of holographic imaging*, Ph. D. Thesis, Ohio State University, 1967.
[6] JAGOSZEWSKI E., KLAKOČAR-CIEPACZ M., Optik **72** (1986), 165.
[7] JAGOSZEWSKI E., Optik **83** (1989), 151.

Received March 22, 1990
in revised form June 28, 1990

Применение сферического голографического элемента для реализации преобразования Фурье

Представлен оптический голографический элемент в применении для реализации преобразования Фурье. В результате интерференции плоской волны отнесения со сферической предметной волной образовалась аксиальная голограмма на сферической основе. В таком случае плоские волны, распространяющиеся в разных направлениях и представляющие разные значения простанственных частот, могут при помощи такого голографического элемента концентрироваться в виде спектра Фурье.

Перевел Станислав Ганцаж